ACS Catalysis

Research Article

pubs.acs.org/acscatalysis

Correlation between Hydrocarbon Product Distribution and Solvent Composition in the Fischer–Tropsch Synthesis Catalyzed by Colloidal Cobalt Nanoparticles

Jorge A. Delgado,[†,‡] Carmen Claver,*[,†,‡] Sergio Castillón,[§] Daniel Curulla-Ferré,[∥] and Cyril Godard*[,‡]

[†]Centre Tecnològic de la Química, C/Marcel.li Domingo s/n, Building N5, 43007, Tarragona, Spain

[‡]Departament de Química Física i Inorgànica and [§]Departament de Química Analítica i Orgànica, Universitat Rovira I Virgili, C/Marcel.li Domingo s/n, 43007 Tarragona, Spain

[∥]Total Research and Technology Feluy, Zone Industrielle Feluy C, B-7181 Seneffe, Belgium

Supporting Information

ABSTRACT: Colloidal cobalt nanoparticles with well-defined particle size (ca. 2.7 nm) were synthesized, characterized, and tested in Fischer–Tropsch synthesis (FTS) using water and binary mixtures as solvent. The catalytic results revealed that activity and selectivity strongly depend on the nature and composition of the solvent mixture: the tests in pure water produced light hydrocarbons (C_2–C_4), while the addition of organic cosolvents increased the activity and shifted the selectivity to higher hydrocarbons (C_{13}–C_{30}). The observed variations in the activity and selectivity were correlated to syngas solubility in the medium used for catalysis. Under the tested conditions, ethanol/water (93/7 v/v) appeared to be the optimum binary solvent in terms of FT activity.

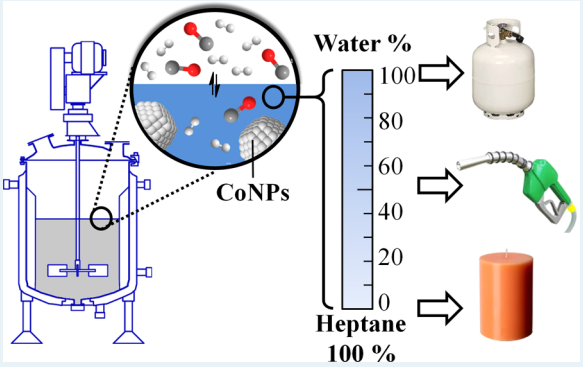

KEYWORDS: *Fischer–Tropsch, cobalt nanoparticles, solvent effect, solvent mixtures, product distribution, hydrocarbon selectivity, chemical reduction, thermal decomposition, polyvinylpyrrolidone*

INTRODUCTION

Due to the fluctuating price of crude oil, Fischer–Tropsch synthesis has generated renewed scientific interest because of its potential capacity to produce high quality synthetic fuels.[1] Through this reaction, synthesis gas (a mixture of carbon monoxide and hydrogen) is transformed into a series of linear hydrocarbon products.[2] At the same time, synthesis gas can be produced from alternative feedstocks such as coal, natural gas, and more recently biomass, making this transformation a key process of the solid-to-liquids (STL), gas-to-liquids (GTL), and biomass-to-liquids (BTL) technologies.[3]

Currently, one of the main challenges in FT research is the design of not only active and stable catalysts but also highly selective active phases that provide hydrocarbons with narrow chain length distributions.[4] Among the parameters that were shown to affect the selectivity of FT catalysts, the conditions used (T, P, H_2/CO ratio), the particle size of the catalysts, and the presence of additives at the catalyst surface are probably the most relevant.[5] The presence of FT products (water and hydrocarbons) at the catalyst surface was also reported to influence the output of the reaction.[6] For instance, Van Steen and Claeys reported the effect of the presence of small amounts of water during Fischer–Tropsch synthesis using a supported ruthenium catalyst suspended in squalane in a slurry reactor.[6b] This study showed that the addition of water during catalysis led to a significant increase in product formation rates and to relevant variations in hydrocarbon selectivity, in particular lower methane selectivity and improved chain growth.

The effect of other solvents in Fischer–Tropsch synthesis was also identified in several reports as a key parameter to enhance the catalytic performance of the catalysts. Liu et al. studied the influence of additional linear hydrocarbons on the selectivity to α-olefin products in FTS using a supported Co catalyst in a fixed-bed reactor system.[7] With these solvents, no relevant effect on the catalytic activity nor the chain growth probability (α-value) was observed, although a significant decrease in selectivity to α-olefins was described when long chain hydrocarbon solvents such as hexadecane were used. The same group reported the effect of solvent on the selectivity to long chain linear α-olefins over cobalt Fischer–Tropsch catalysts.[8] Interestingly, ca. 40% selectivity to α-olefins was obtained in the presence of *n*-decane, in comparison to ca. 2% in the presence of *n*-hexane and it was concluded that hydrogenation of α-olefins is more efficient in *n*-hexane.[5] According to the authors, this phenomenon indicates that the primary α-olefin products can be more effectively removed

Received: December 18, 2014
Revised: May 20, 2015
Published: May 28, 2015

DOI: 10.1021/cs5020332
ACS Catal. 2015, 5, 4568–4578

from the catalyst bed in *n*-decane due to the higher affinity for heavy aliphatic hydrocarbons expected for this solvent according to the longer carbon chain in comparison to *n*-hexane.

The Davis group also investigated the effect of solvent on the performance of supported cobalt-based catalysts in Fischer–Tropsch synthesis using a continuously stirred tank reactor.[9] They observed an increase in conversion when the molecular weight of the solvent decreased. According to the authors, the decrease in conversion with time is likely to be a result of pore filling with solvent into the interior of the catalyst, which increases with increasing molecular weight of the start-up solvent.

For the study of solvent effects in FTS, the use of unsupported nanoparticles is of high interest due to the suppression of support-related issues such as internal mass transport. Moreover, the synthesis of nanocatalysts by colloidal methods provides a better control of their size and shape compared to that of classical supported heterogeneous catalysts. The first example of colloidal nanoparticles applied as catalysts in aqueous FT synthesis (AFTS) was reported by Xiao et al., who used ruthenium nanoclusters stabilized by poly(*N*-vinyl-2-pyrrolidone) (PVP).[10] Using these nanocatalysts, they described a 35-fold increase in the activity over traditional supported Ru catalysts. The smaller size and high dispersion, and the three-dimensional freedom of the particles in water were discussed as the key factors for such an increase in catalytic activity at 180 °C. In addition, as the products of FTS are insoluble in water, they can be easily separated from the reaction mixture.[11] The same authors later reported the effect of ionic additives on the performance of these colloidal catalysts.[12] The same catalyst was also tested by Quek et al. in the low temperature AFTS and a high selectivity to oxygenates was obtained. The authors attributed this effect to a higher CO coverage at the NP surface under these conditions.[13] Recently, our research group reported the catalytic performance of colloidal Ru-NPs stabilized by various polymers such as PVP and lignins and showed that the nature of the NPs stabilizers influences the selectivity of Ru catalysts in AFTS.[14]

Concerning cobalt catalysts, Wang et al. recently reported the use of cobalt/platinum alloy nanoparticles stabilized by PVP as catalysts of the AFTS.[11] According to this report, activity up to 1.1 mol_{CO} $mol_{Suf\text{-}Co}^{-1}$ h^{-1} with a growth factor (α) of 0.8 was obtained at 160 °C. This outstanding activity was rationalized by the formation of Co overlayer structures on Pt NPs or Pt–Co alloy NPs. The same authors tested Co nanoparticles reduced by $LiBEt_3H$ and $NaBH_4$, in the aqueous-phase Fischer–Tropsch synthesis.[15] Better catalytic performance was observed for the former case, and comparing the particle size distribution of the catalysts before and after reaction, it was suggested that catalyst reconstruction occurs during the reaction. In addition, it was proposed the B-doping could affect the catalytic performance of these NPs. In a previous study, Fan et al. reported an activity of 0.12 mol_{CO} mol_{Co}^{-1} h^{-1} at 170 °C in the AFTS for CoNPs synthesized by chemical reduction using sodium borohydride as reducing agent in water.[16] Other colloidal Co nanocatalysts for FTS were reported in ionic liquids[17] and squalane[18] although in these cases generally low activity and agglomeration issues were described. Dupont and co-workers reported the synthesis of Co nanocubes (54 ± 22 nm)[17a] and nanospheres (7.7 ± 1.2 nm)[17b] by thermal decomposition of $Co_2(CO)_8$ in [DMI]-[NTf_2] and [BMI][NTf_2], respectively. The obtained materials resulted in active catalysts for FTS. Very recently, the same author reported the synthesis of bimetallic Co/Pt NPs in [BMI][PF_6], this time through an organometallic approach.[19] The isolated bimetallic NPs resulted in active catalysts for the Fischer–Tropsch synthesis, with selectivity for naphtha products.

Nowadays, while the activity of FT catalysts can be efficiently tuned by several parameters such as the type of support or the addition of promoters, the control of the selectivity for a selected hydrocarbon fraction is less documented and remains a challenge.[20] The study of parameters that could shift the product distribution in FT is therefore of high interest for the rational design of catalytic systems providing selectively diesel or gasoline fractions, for instance.

Here, we describe the synthesis and characterization of monometallic CoNPs stabilized with poly(*N*-vinyl-2-pyrrolidone) and their application as nanocatalysts in FTS. The effect of solvent composition on the catalytic performance of these NPs was investigated. Varying the composition of the solvent caused striking effects on the product distribution of the reaction from light to heavier hydrocarbons, which were correlated to the relative CO and H_2 solubility under these reaction conditions.

EXPERIMENTAL SECTION

Synthesis of Cobalt Nanoparticles by Chemical Reduction Method (Co1). Co1 was synthesized by chemical reduction of cobalt(II) chloride in the presence of polyvinylpyrrolidone (PVP) as stabilizer (PVP:Co ratio of 20) using sodium borohydride as reducing agent. As a standard procedure, 0.226 g of $CoCl_2{\cdot}6H_2O$ (0.93 mmol) was dissolved in 50 mL of H_2O containing the 2.066 g of PVPK30 (18.6 mmol based on monomer units, PVP:Co ratio of 20). Then, a solution of 0.358 g of $NaBH_4$ (9.30 mmol) in 16 mL of H_2O was added at room temperature during 5 min. The solution was maintained under vigorous mechanical stirring for 2 h. Then 100 μL of the colloidal solution was centrifuged, washed with water and redispersed by sonication. Three drops of the obtained colloidal solution were deposited on a Cu-Formvar or holey carbon grids for TEM and HR-TEM analysis. For the isolation of the CoNPs, the freshly prepared NPs were initially precipitated by a strong magnetic field (using a neodymium magnet) and the supernatant was decanted. Then, the precipitated NPs were washed with water to remove the excess of salts and PVP. The decantation and washing process was repeated three times with water, then three times with ethanol and three times with hexane. The resulting CoNPs were finally dried under vacuum and stored in a glovebox.

Synthesis of Cobalt Nanoparticles by a Thermal Decomposition Method (Co2). Co2 was synthesized by thermal decomposition of $Co_2(CO)_8$ in the presence of the PVP (PVP:Co ratio of 10) using butylether as solvent. As a standard procedure, 0.352 g of $Co_2(CO)_8$ (1.86 mmol) and 2.066 g of PVP (18.6 mmol based on monomer units, PVP:Co ratio of 10) were placed in a 500 mL Fischer–Porter bottle and dissolved with 130 mL of butyl ether. The Fischer–Porter bottle was closed and then heated at 150 °C during 2 h to give a black suspension. The CoNPs were then precipitated using a strong magnet and the solvent was decanted. The CoNPs were washed with butylether, followed by THF and hexane and finally dried under vacuum and stored in a glovebox. For the purpose of characterization, a fraction of the isolated NPs was washed with water in order to remove any PVP excess, followed

DOI: 10.1021/cs5020332
ACS Catal. 2015, 5, 4568–4578

by ethanol and hexane washing prior to vacuum drying and storage in a glovebox. Samples of **Co2** were centrifuged, washed with water and redispersed by sonication several times. Three drops of the obtained colloidal solution were deposited on a Cu-Formvar or holey carbon grids for TEM and HR-TEM analysis.

General Method for Fischer–Tropsch Catalytic Experiments. In a typical catalytic experiment, freshly prepared CoNPs (0.931 mmol of Co) were redispersed in the desired solvent and the suspension placed in a Teflon liner within a 100 mL stainless steel autoclave which was purged three times with Ar, and pressurized at an Ar pressure of 1.5 bar. An additional 10 bar of CO and 20 bar of H_2 were further added giving a final pressure of 31.5 bar (H_2:CO:Ar = 2:1:0.15). The autoclave was then heated to 180 °C under mechanical stirring at 1000 rpm during 12 h. At this point, the autoclave was cooled to room temperature prior to gas analysis. All the components contained in the gas phase (CO, H_2, Ar, CO_2, and C_1–C_8 hydrocarbons) were analyzed by GC-TCD and the quantification was performed using calibration curves for each component. The compounds present in the liquid phase were analyzed directly from the hydrocarbon phase or extracted with cyclohexane (10 mL) containing 1 μL of bicyclohexyl as internal standard. The organic phase containing the hydrocarbon and oxygenated products were analyzed by GC-MS. The identification and quantification of products was performed by comparison with standards using calibration curves for each compound.

RESULTS AND DISCUSSION

Synthesis and Characterization of CoNPs. The cobalt nanoparticles **Co1** were synthesized in water by chemical reduction of $CoCl_2 \cdot 6H_2O$ in the presence of $NaBH_4$ using PVP as stabilizer (PVP:Co = 20) while **Co2** were produced by thermal decomposition of $Co_2(CO)_8$ in butylether at 150 °C in the presence of 10 equiv of PVP. In this latter case, the amount of PVP was lower than for the chemical reduction method due to solubility issues. Both methodologies are represented in Scheme 1.

Scheme 1. Methodologies Used for the Synthesis of CoNPs Co1–Co2

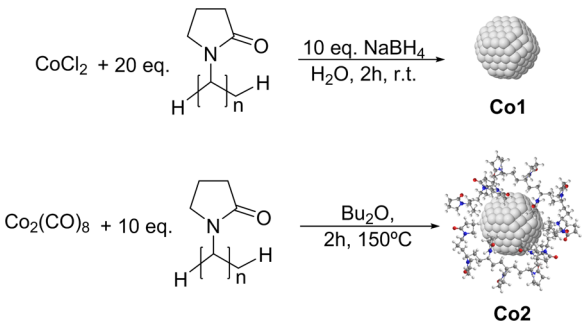

According to the TEM micrographs and size histograms of **Co1** and **Co2** displayed in Figure 1, both methodologies resulted in the formation of spherical CoNPs of similar sizes ca. 2.7 nm (**Co1** 2.64 ± 0.92 nm; **Co2** 2.78 ± 0.71 nm).

The fine structure of the CoNPs **Co1** and **Co2** was studied by high-resolution transmission electron microscopy (HR-TEM). The corresponding micrographs are displayed in Figure 2, where the insets represent the electron diffraction patterns of the NPs. In the micrograph of **Co1** (Figure 2, left), single particles of ca. 2.6 nm diameter were observed, in agreement with TEM measurements. Analysis of the diffraction pattern revealed the presence of crystalline Co_3O_4-fcc (space group *Fd*3*m*(227)). Curiously, no crystalline metallic cobalt phase was identified. The diffuse rings present in the electron diffraction pattern of these NPs suggest an amorphous structure for the cobalt faces, in agreement with previously reported synthesis of amorphous CoNPs via similar synthetic methods.[21]

In contrast, the analysis of the diffraction pattern of **Co2** revealed the presence of crystalline Co-hcp (space group *P*63/*mmc*) while crystalline cobalt oxides were not detected in this case.

When the crystalline structure of the CoNPs was studied using X-ray diffraction (XRD) technique, the XRD pattern of **Co1** revealed the presence of two broad bands centered at 34° and 45° which cannot be unambiguously attributed to any defined crystalline pattern (Figure 3). In contrast, in the diffractogram of **Co2**, low intensity peaks were observed at 42, 45, 47, and 76° which were readily attributed to Co-hcp and Co-fcc crystalline phases. The broad feature at 20 degrees observed for **Co2** was attributed to the 89 wt % of PVP that covers the CoNPs surface. This was confirmed by XRD analysis of a sample of **Co2** previously washed with water that revealed an important decrease of this band due to the partial removal of PVP (see the Supporting Information). These results therefore indicate that the synthetic method used for the formation of NPs affects the crystalline structure of Co.

Surface analysis of the CoNPs **Co1** and **Co2** was performed by X-ray photoelectron spectroscopy (XPS). The full XPS spectra of **Co1** revealed the presence of Na, Co, O, N, C, and B, according to the peaks observed at their characteristic binding energies (1071.6, 781.5, 530.9, 399.2, 284.5, and 191.1 eV, respectively). The Co XPS spectrum of **Co1** exhibits two prominent peaks at 779.7 and 795.6 eV corresponding to Co $2p_{3/2}$ and Co $2p_{1/2}$, respectively. A low intensity shoulder detected at 777.9 eV can also be distinguished and suggests the presence of a cobalt metal phase (ca. 37% of Co^0 according to deconvolution of the Co XPS spectra). It was therefore concluded that partial oxidation of these NPs occurred during their synthesis, probably due to the presence of oxygen dissolved in water. In contrast, for **Co2**, only characteristic peaks of PVP (O, N, and C) were detected in the full XPS spectra, suggesting again the abundant coverage of **Co2** by PVP, and therefore no information about the reduction state of cobalt at the metal surface could be obtained from this technique. Further analysis of **Co1** by ICP revealed a boron content of 5.9 wt %, which corresponds to a Co/B ratio of 2.8.

The presence of PVP at the surface of these CoNPs was also investigated by FTIR, TGA, and ICP-OES techniques. The IR spectra of **Co1** did not exhibit absorption bands of PVP whereas for the case of **Co2**, characteristic absorption bands of PVP at 3460, 2955, and 1663 cm^{-1} were detected. To quantify the exact cobalt content of these NPs, ICP-OES analyses were performed, obtaining 82.4 and 5.8 wt % for **Co1** and **Co2**, respectively, in agreement with the weight losses observed by TGA. These results therefore confirmed that the coverage of the surface of these NPs by PVP is also affected by the synthetic method used for their formation, and is much more important in the case of **Co2** than in that of **Co1**. Due to the large excess of PVP remaining at the surface of **Co2**, a sample was washed with water and subsequently analyzed by FTIR and TGA (Supporting Information). For **Co2**, characteristic peaks of PVP at 2955 and 1663 cm^{-1} corresponding to CH and CO

DOI: 10.1021/cs5020332
ACS Catal. 2015, 5, 4568–4578

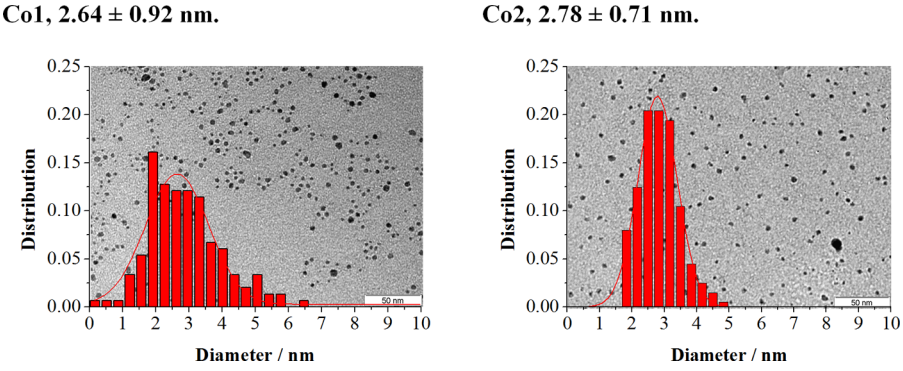

Figure 1. Size histograms and TEM micrographs of **Co1** and **Co2**.

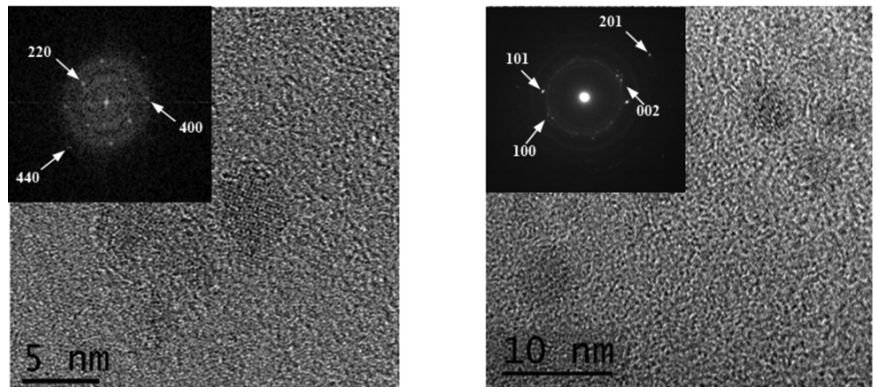

Figure 2. HRTEM image of **Co1** (left) and **Co2** (right) NPs and their corresponding electron diffraction patterns.

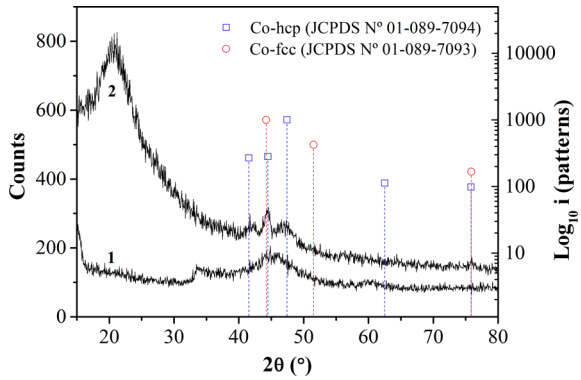

Figure 3. XRD patterns of (1) **Co1** and (2) **Co2**.

stretching vibrations, respectively, were still observed thus indicating the presence of remaining polymer at the NPs surface. Additionally, a weight loss of 13% of PVP was determined by TGA thus demonstrating the coordination of PVP at the surface of **Co2** after water washing.

In summary, the characterization of **Co1** and **Co2** NPs revealed that the composition and structure of these CoNPs depend strongly on the synthetic methodology used for their formation. Despite both **Co1** and **Co2** showing similar particle size (ca. 2.6 nm), **Co1** NPs are constituted of cobalt and boron phases with an amorphous structure, while **Co2** is metallic cobalt with hcp and fcc crystalline phases. Furthermore, relevant differences in PVP coverage were observed and showed that **Co1** is poorly wrapped by PVP compared to **Co2**.

Fischer–Tropsch Catalytic Experiments. The synthesized Co NPs (**Co1** and **Co2**) were tested in the Fischer–Tropsch synthesis using various solvents (monocomponent or binary mixtures) in order to study the effect of solvent on the activity and selectivity of the CoNPs.

Catalysis in Water. The synthesized NPs **Co1** were first tested in AFTS using water as solvent at 150, 180, and 210 °C under 30 bar of syngas (Table 1). Activity increased from 0.012

Table 1. Fischer–Tropsch Synthesis Catalyzed by Co1 and Co2 Using Water As Solvent[a]

			selectivity, wt %			hydrocarbon sel., wt %			
E[b]	temp (°C)	activity[c]	CO_2	CH_4	C_{2+}	C_{2-4}	C_{5-12}	C_{13-30}	α
1	150	0.012	44	8	48	41	45	0	0.60
2	180	0.026	23	20	57	43	31	0	0.59
3	210	0.097	54	25	21	30	16	0	0.50
4[d]	180	0.205	23	27	50	41	24	0	0.57

[a]Reaction conditions: 30 bar H_2/CO/Ar (2:1:0,15), 66 mL water, 1000 rpm, 12h. [b]**Co1** (0.93 mmol Co). [c]Activity without CO_2 in mol_{CO} mol_{Co}^{-1} h^{-1}. [d]**Co2** (0.93 mmol Co).

to 0.097 mol_{CO} mol_{Co}^{-1} h^{-1} as the temperature increased from 150 to 210 °C (note: CO_2 was not considered for the activity calculation). Methane selectivity steadily increased from 8 to 25 wt % as temperature increased, whereas C_{2+} selectivity initially increased from 48 wt % at 150 °C to 57 wt % at 180 °C, but decreased to 21% when temperature was further increased to 210 °C. The rise in temperature also caused a considerable shortening of the hydrocarbon chain (decrease of the α value from 0.60 to 0.50) and favored the methanation reaction, in agreement with trends previously reported for cobalt catalysts.[5]

For **Co2**, an activity of 0.205 mol_{CO} mol_{Co}^{-1} h^{-1} was observed at 180 °C with a selectivity of 27% for methane and

DOI: 10.1021/cs5020332
ACS Catal. 2015, 5, 4568–4578

Table 2. Screening of Mixtures of Organic Solvents with Water (15%) in the Fischer–Tropsch Synthesis Catalyzed by Co1[a]

				selectivity, wt %			hydrocarbon sel., wt %			
E[b]	solvent (% v/v)	bp, °C	activity[c]	CO_2	CH_4	C_{2+}	C_{2-4}	C_{5-12}	C_{13-30}	α
1	water (100%)	100	0.026	23	20	57	43	31	0	0.59
2	heptane (15%)	99	0.067	23	11	66	7	19	59	0.92
3	methylcyclohex (15%)	101	0.058	19	15	66	11	22	49	0.92
4	toluene (15%)	111	0.071	20	12	68	10	22	53	0.91
5	perfluorooctane (15%)	103	0.076	10	10	80	11	21	57	0.91
6	propanol (15%)	98	0.052	19	18	63	37	28	13	0.79

[a]Conditions: 0.93 mmol Co, 30 bar H_2/CO/Ar (2:1:0,15), 66 mL total volume, 1000 rpm, 180 °C, 12 h. [b]**Co1** (0.93 mmol Co). [c]Activity without CO_2: mol_{CO} mol_{Co}^{-1} h^{-1}.

50% for C_{2+}. The activity of **Co2** was ca. 10 times higher than that of **Co1** at this temperature and was attributed to the higher reduction degree of **Co2**. In contrast, the product selectivities observed for **Co1** and **Co2** were quite similar at 180 °C, indicating that under these conditions, the differences in structure and composition of these CoNPs do not affect significantly the selectivity of the reaction. The obtained activities for **Co1** and **Co2** are comparable to those recently reported by Wang et al. in the AFTS catalyzed by CoNPs (0.27 and 0.1 mol_{CO} mol_{Co}^{-1} h^{-1} corresponding to NPs prepared by chemical reduction using $NaBH_4$).[15] The hydrocarbon selectivities as well as the α values observed in water were also comparable. The CH_4 and CO_2 selectivities obtained in this study were 20 and 23 wt % differently to the values reported by Kou, 40 and 7 wt % respectively. These differences could be attributed not only to variations in the structure of the catalysts but also to the composition (extent of B-doping).

It is noteworthy that in these catalytic experiments, most of the hydrocarbon products were in the C_{1-4} fraction and no products longer than C_{12} were obtained. Usually, the range of α for Co-catalyzed FTS is ca. 0.70–0.80 depending on the reaction conditions and catalyst type.[22] Here, using water as solvent, α values of 0.50–0.60 were obtained in all cases. This significant difference in selectivity may indicate that water is responsible for the shortening of the hydrocarbon chain, possibly due to the low solubility of syngas in water.[23]

Catalysis in Mixtures of Water and Organic Cosolvent. In view of these results, it was thought that the addition of an organic cosolvent could exert a direct effect on the selectivity of AFTS. Therefore, catalytic experiments using mixtures of water and a series of organic solvents (15% v/v) were carried out (Table 2). The organic cosolvents were selected on the basis of their boiling point (similar to that of water), to minimize vapor pressure effects during catalysis. For this initial screening, aliphatic (linear and cyclic), aromatic and perfluorinated hydrocarbons and alcohols were tested.

When a 15% v/v of heptane/water was used as the solvent mixture, the activity of the **Co1** NPs at 180 °C increased up to 0.067 mol_{CO} mol_{Co}^{-1} h^{-1} (× 2.5 compared to that obtained in pure water) with a clear shift of the hydrocarbon selectivity from C_{2-4} to C_{13-30} (Table 2, entry 2 vs entry 1). Furthermore, a significant decrease of the methane and CO_2 selectivities, to 11% and 23% respectively, was also observed (Table 2, entry 2). In methylcyclohexane and toluene (entries 3 and 4), similar results were obtained with activities of ca. 0.06–0.07 mol_{CO} mol_{Co}^{-1} h^{-1}, together with high selectivities to C_{13-30} and low selectivities to methane and CO_2.

Hydrogenation of toluene was not observed when the FT catalysis was performed in this aromatic solvent. The catalysis in perfluorooctane (entry 5) gave the highest activity of the series, up to 0.076 mol_{CO} mol_{Co}^{-1} h^{-1}, the highest C_{2+} selectivity (80%), and the lowest CO_2 and CH_4 selectivities (10% for both). Long chain hydrocarbons (C_{13+}) were again the main reaction products under these conditions.

When the catalysis was performed in 15% v/v of propanol/water (entry 6), intermediate results between those in water and heptane (15% v/v) were obtained. It is noteworthy that the hydrocarbon selectivity increased in the order water < heptane < perfluorooctane, suggesting that these variations could be caused by the increased solubility of H_2 and CO in these solvents.[23,24]

To summarize, when the catalysis was performed in water the growth of the hydrocarbon chain was restricted to C_{1-12} products whereas upon addition of 15% of an organic cosolvent such as heptane, catalytic activity increased, and chain lengthening was observed (C_{13}–C_{30}).

In view of the results obtained with this series of cosolvents, and since water and hydrocarbons are products of the FTS reaction, the composition of the water/heptane mixture was optimized.

Optimization of the Composition of Water/Heptane Mixtures. To further investigate the effect of the cosolvent, the water/heptane mixture was investigated at various heptane contents.

In these experiments, increasing the heptane content resulted in an increase in the activity of **Co1** (Figure 4, solid line) up to a maximum of 0.095 mol_{CO} mol_{Co}^{-1} h^{-1} at v/v 50%; however, the activity decreased to 0.009 mol_{CO} mol_{Co}^{-1} h^{-1} as heptane content was further increased. The same behavior was observed for **Co2** (Figure 4, dotted line) although much higher activities (up to 0.27 mol_{CO} mol_{Co}^{-1} h^{-1}) than those for **Co1** were

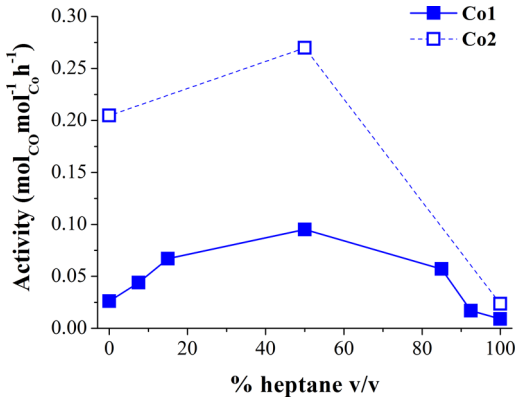

Figure 4. Activity (mol_{CO} mol_{Co}^{-1} h^{-1}) of **Co1** and **Co2** NPs as a function of the percent heptane in water. Conditions: 0.949 mmol Co, 30 bar H_2/CO/Ar (2:1:0,15), 66 mL water, 1000 rpm, 180 °C, 12 h.

DOI: 10.1021/cs5020332
ACS Catal. 2015, 5, 4568–4578

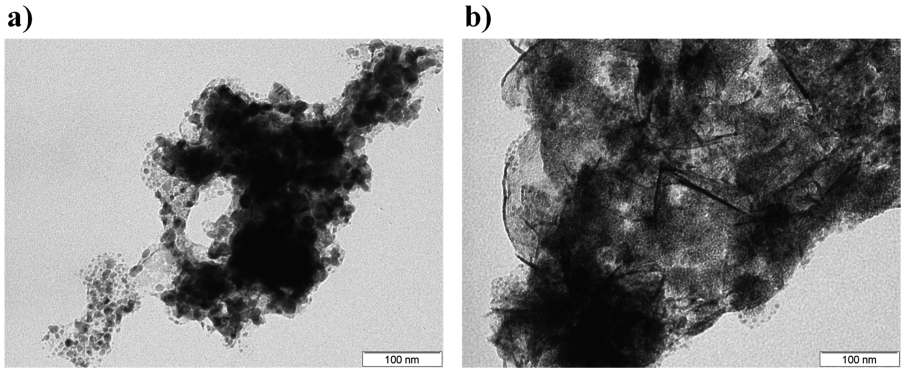

Figure 5. TEM micrographs of (a) **Co1** and (b) **Co2** after catalysis performed in heptane as the solvent.

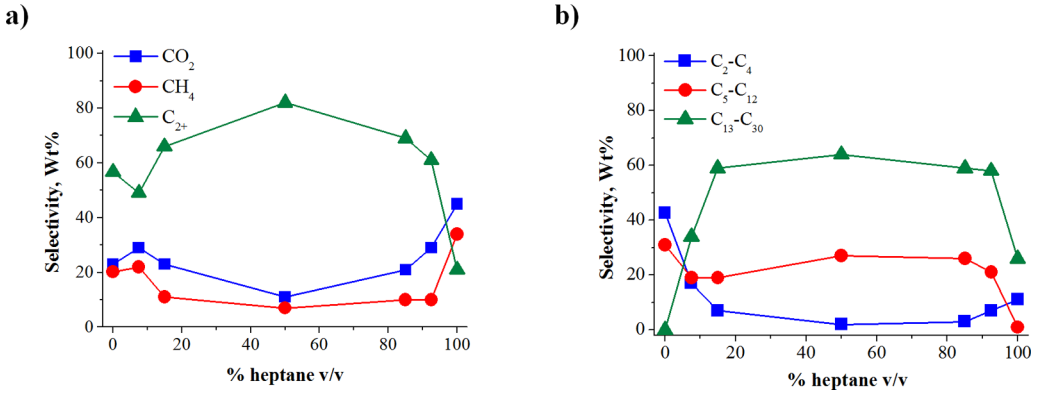

Figure 6. Selectivity (a) and hydrocarbon selectivity (b) in wt % of **Co1** NPs as a function of the heptane content in the solvent used for catalysis. Conditions: 0.949 mmol Co, 30 bar H_2/CO/Ar (2:1:0,15), 66 mL water, 1000 rpm, 180 °C, 12 h.

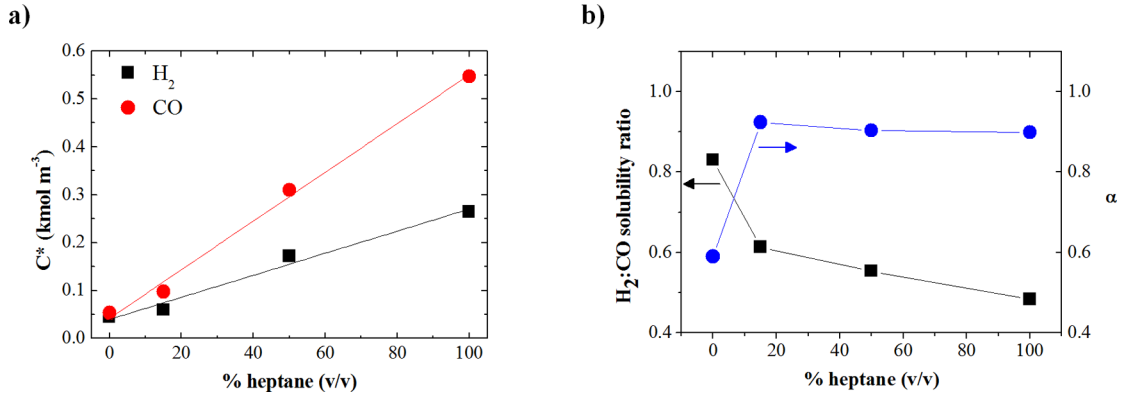

Figure 7. (a) Solubility of H_2 and CO at 20 and 10 bar, respectively, and rt in heptane/water mixtures. (b) Measured H_2:CO solubility ratio and α values obtained in catalysis using different heptane/water mixtures.

measured. The higher activity of **Co2** can be attributed to the higher reduction degree of the **Co2** catalyst, as previously indicated.

On the other hand, at high heptane content, important agglomeration of **Co1** and **Co2** was observed by TEM analysis performed after the catalytic tests. The low activity observed for both catalysts at high heptane content was therefore explained by the agglomeration of the nanocatalysts in such an apolar solvent (Figure 5).

The selectivity was also strongly affected by the composition of the solvent. The selectivity profiles for **Co1** as a function of the heptane/water ratio are displayed in Figure 6a. The hydrocarbon selectivity (C_{2+}) increased up to 82% when the heptane content was increased to 50%. Simultaneously, the CO_2 and CH_4 selectivities decreased from 23 to 11% and from 20 to 7%, respectively. At higher heptane contents, C_{2+} selectivity decreased down to 21% while CO_2 and CH_4 both increased to 45 and 34%, respectively. In 50/50 heptane/water mixture, the use of **Co2** as catalyst provided slightly higher selectivities to hydrocarbons (84%, Supporting Information).

The hydrocarbon product distribution was also considerably affected when the heptane content in the solvent mixture was varied (Figure 6b). The variation of solvent composition from pure water to a water/heptane mixture of 85/15 caused a strong shift of the product distribution from C_2−C_{12} toward the heavy fraction C_{13-30} (Figure 6b), which is reflected in the increase of α value from 0.59 to ca. 0.90. This level of selectivity

DOI: 10.1021/cs5020332
ACS Catal. 2015, 5, 4568−4578

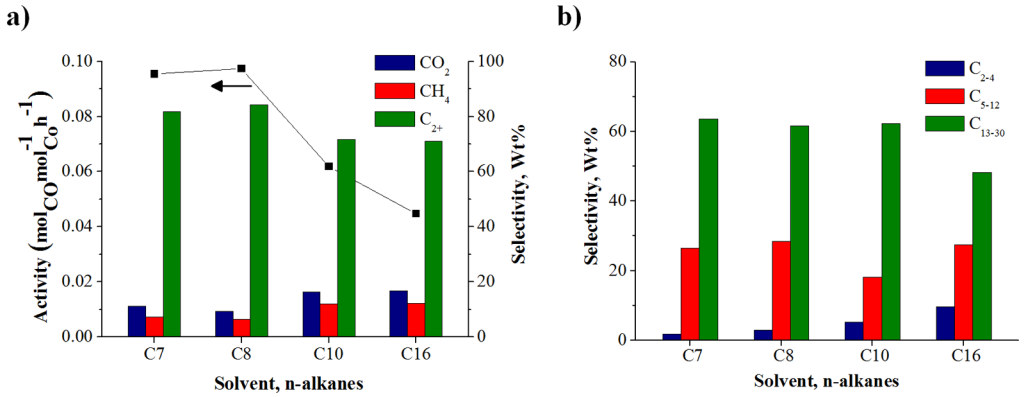

Figure 8. Activity and selectivity (a) and hydrocarbon selectivity (b) in wt % of **Co1** NPs as a function of the carbon chain length of the alkane cosolvent. Conditions: 0.949 mmol Co, 30 bar H_2/CO/Ar (2:1:0,15), 66 mL water, 1000 rpm, 180 °C, 12 h.

remained constant at heptane contents between 15 and 93% and dropped drastically when pure heptane was used as solvent.

The selectivity drop observed for pure heptane was attributed to the agglomeration of the NPs described above (Figure 5). It is also noteworthy that no C_{30+} products were detected in these experiments. Similar trends were observed for **Co2** (Supporting Information).

The dependence of the activity on the percentage of heptane in water can be rationalized by the variation of the solubilities of hydrogen and carbon monoxide in the different solvent mixtures. According to literature data, the solubility of hydrogen is higher in decane than in water by a factor of ca. 7 (3.348 mLH_2/L[25] vs 0.488 mLH_2/L[23]) under reaction conditions (180 °C and 20 bar of H_2). A higher solubility in heptane would represent a higher coverage of the metal surface by both gases, resulting in an increase in the activity when the heptane content increases from 0 to 50%. The shift in product distribution from C_{2-4} to C_{13+} could also be explained by the increase solubility of syngas.

To confirm this hypothesis, the solubilities of H_2 and CO were measured in various heptane/water mixtures at room temperature using the method described by Deimling et al.[26] The results are displayed in Figure 7a. Solubility of both gases increased linearly as the heptane content increased. In all cases, CO solubility was higher than that of H_2 and the H_2:CO solubilities ratio (Figure 7a) decreased at higher heptane content. Interestingly, an inverse correlation was observed between the variation in H_2:CO solubility ratio and the chain growth probability of the FT products (Figure 7b). Indeed, when the heptane content is increased from 0 to 15%, a drastic drop in H_2:CO ratio is observed, and concomitantly, an increase in the α value was measured. At higher heptane content, the H_2:CO solubilities ratio is less affected, which is reflected in an almost constant α value. From these results, it was concluded that the variations observed in hydrocarbon product distribution were mainly controlled by the H_2:CO ratio in solution. At low H_2:CO solubilities ratio, long chain hydrocarbons are formed (C_{13+}) while at higher ratios, lighter hydrocarbons are preferably produced. These results are in agreement with previous reports which described that variations of the syngas composition affect the product distribution in FTS.[5]

These results therefore indicate that the presence of water and hydrocarbon at the surface of cobalt nanocatalysts produced by FTS strongly influences their subsequent selectivity by affecting the solubility of syngas and the CO coverage of these catalysts. The results described here suggest that the presence of water at the NP surface shortens the chain of the hydrocarbon products. XPS analysis of the used catalysts is displayed in the Supporting Information. The phase separation in water/heptane solvent mixtures was qualitatively studied through optical measurements of the flow regime in a transparent model reactor (Supporting Information). Using 15 or 50% heptane/water mixtures, homogeneous oil-in-water emulsions were observed. In contrast, using 85% heptane/water mixture, a water-in-oil emulsion was formed, and the drops of the aqueous phase inside heptane were this time appreciable.

Next, to investigate the effect of the carbon chain length of the cosolvent on the selectivity, a series of mixtures of hydrocarbons and water was tested as media for the Fischer–Tropsch reaction.

Screening of Hydrocarbons As Cosolvents (50% v/v). In view of the results obtained with the 50% v/v heptane/water mixture, the effect of the hydrocarbon chain length was studied with solvent mixtures composed of water and *n*-octane, *n*-decane, and *n*-hexadecane in the same proportions (Figure 8).

The catalytic tests using heptane or octane in 50% v/v showed similar activity; however, activity decreased as chain length further increased in the series from octane to hexadecane. The activity observed for hexadecane was half (0.045 $mol_{CO}\ mol_{Co}^{-1}\ h^{-1}$) of that observed for heptane (0.095 $mol_{CO}\ mol_{Co}^{-1}\ h^{-1}$). Agglomeration was not observed in any case, and TEM images showed that dispersion of the CoNPs was similarly independent of the cosolvent. This decrease in the activity was therefore attributed to the lower solubility of syngas in heavier *n*-alkanes, as previously reported.[25]

In terms of selectivity, the amount of methane and CO_2 formed during the reactions slightly increased with longer chain cosolvents. Simultaneously, only a small shift toward lighter products was observed for octane and hexadecane, although it became more relevant for hexadecane. These small variations in selectivity could be attributed to the expected similarity of the H_2/CO ratio in these media. Interestingly, these trends are in contrast with those previously reported for supported CoNPs on SiO_2, for which no changes in the activity nor in chain growth probability were observed when the same series of solvents were tested in slurry-type FT systems.[7]

Screening of Alcohols As Solvents for FTS. According to the initial screening of solvents (Table 2), the extent of chain growth in propanol/water mixture was a somewhat intermediate between those obtained in water and heptane/water, according to their α values (0.79, 0.59, and 0.92 respectively).

DOI: 10.1021/cs5020332
ACS Catal. 2015, 5, 4568–4578

This suggested that performing the catalytic reaction in alcohols could be of interest for the modulation of the product distribution. Moreover, alcohols have the capacity to disperse efficiently CoNPs such as **Co1** and **Co2**, even in the absence of water.

It was therefore decided to investigate the effect of various alcohols and catalytic experiments using the series methanol, ethanol, 1-propanol, 1-butanol, and 1-pentanol were performed (Table 3). The results of these experiments showed that when the FT reaction is performed in pure alcohols (>C_1), three types of products are formed (Scheme 2): (a) FT products, (b) FT-acetal products formed by reaction of FT intermediate species with two molecules of solvent, and (c) C_n-acetals formed from 3 molecules of solvent and where C_n is the carbon number contained in the alcohol structure. The formation of FT-acetal products was previously observed by Fan et al. under FT conditions using ethylene glycol as solvent with the formation of a series of dioxolanes.[27] Here, two different types of acetals were dettected: those involving the reaction of a product formed by FT reaction with two molecules of solvent (route b, Scheme 2) and those formed by reaction of three molecules of solvents (route b, Scheme 2). These acetal products corresponded to less than 1% in alcohol conversion in all cases.

Table 3. Fischer–Tropsch Synthesis Catalyzed by Co1 in Different *n*-Alcohols[a]

		selectivity (%)[b]			
E	alcohol	FT-products	FT-acetals	C_n acetal	final H_2/CO
1	methanol	100	0	0	1.3
2	ethanol	69	13	18	1.8
3	1-propanol	35	35	30	2.1
4	1-butanol	2	44	54	2.7
5	1-pentanol	1	27	73	2.5

[a]Conditions: 0.93 mmol Co, 30 bar H_2/CO/Ar (2:1:0,15), 66 mL total volume, 1000 rpm, 180 °C, 12 h. [b]Selectivity calculated from GC-MS data by peak integration.

The selectivities obtained in these reactions are summarized in Table 3. These selectivities were obtained by integration of the corresponding GC-MS peaks, since no calibration could be performed on these compounds.

Interestingly, among the series of alcohols used, only the FT experiments carried out in methanol produced selectively FT products since no acetals were detected (entry 1). When the solvent was ethanol, ca. 15% of FT-acetals and C_n-acetals were detected (entry 2) while the FT products were still mainly formed. However, when longer chain alcohols were used, an increasing amount of C_n-acetals was produced up to 73% in 1-pentanol with the FT products only detected as traces (entry 5).

The classical mechanism of formation of acetals involves the reaction of one molecule of aldehyde with two molecules of alcohol under acidic conditions with elimination of 1 equiv of water.[28] Recently, Gunanathan et al. reported the use of a homogeneous alcohol dehydrogenation Ru catalyst for the formation of acetals in pure alcohols.[29] In the present case, the role of Co in C_n-acetal formation was confirmed when a blank experiment was performed: when alcohols were heated under the same conditions but in absence of Co catalyst, no acetals were formed. The generation of aldehyde thus requires the presence of Co, and it is proposed that oxidation of one equivalent of alcohol to the corresponding aldehyde proceeds via the concomitant reduction of a cobalt center. Oxidation of the alcohols with H_2 release is supported by the observation of an increase in the H_2:CO ratio in the gas phase when higher amounts of C_n-acetals are formed.

The higher selectivity to C_n-acetals in long chain alcohols can be explained by the lower Gibbs free energy of formation for long chain aldehydes from the corresponding alcohols.[30] Interestingly, when the selectivity to C_n-acetals was plotted against the Gibbs free energy of formation of the aldehyde, a linear relationship was obtained (see the Supporting Information).

These results therefore indicate that when FTS is completed in alcohols as solvents, a competition between the hydrocarbon and acetal formation is observed and depends on the chain length of the alcoholic solvent. This effect is remarkable since, in MeOH, hydrocarbons are mainly formed while, in 1-pentanol, acetals are selectively produced.

Scheme 2. Products Formed under FT Conditions Using Co1 as Catalyst and Alcohols As Solvent

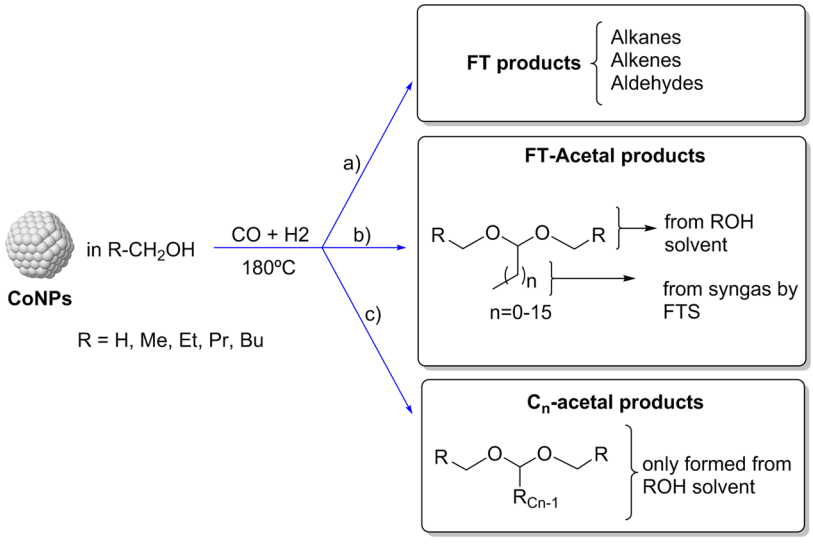

DOI: 10.1021/cs5020332
ACS Catal. 2015, 5, 4568–4578

Table 4. Fischer–Tropsch Synthesis Catalyzed by Co1 Using *n*-Alcohols As Solvent[a]

			selectivity, wt %			hydrocarbon sel.,wt %			
E	alcohol	activity[b]	CO_2	CH_4	C_{2+}	C_{2-4}	C_{5-12}	C_{13-30}	final H_2/CO
1	methanol	0.046	7	8	85	2	21	66	1.3
2	ethanol	0.189	3	5	92	2	26	67	1.8
3	1-propanol	0.053	7	13	80	5	40	42	2.1
4	1-butanol	0.027	13	31	56	14	1[c]	49	2.7
5	1-pentanol	0.043	11	33	56	16	1[c]	46	2.5

[a]Conditions: 0.93 mmol Co, 30 bar $H_2/CO/Ar$ (2:1:0,15), 66 mL total volume, 1000 rpm, 180 °C, 12 h. [b]Activity without CO_2: $mol_{CO}\ mol_{Co}^{-1}\ h^{-1}$. [c]$C_{5-12}$ hydrocarbons overlapped by the solvent peak in GC spectra.

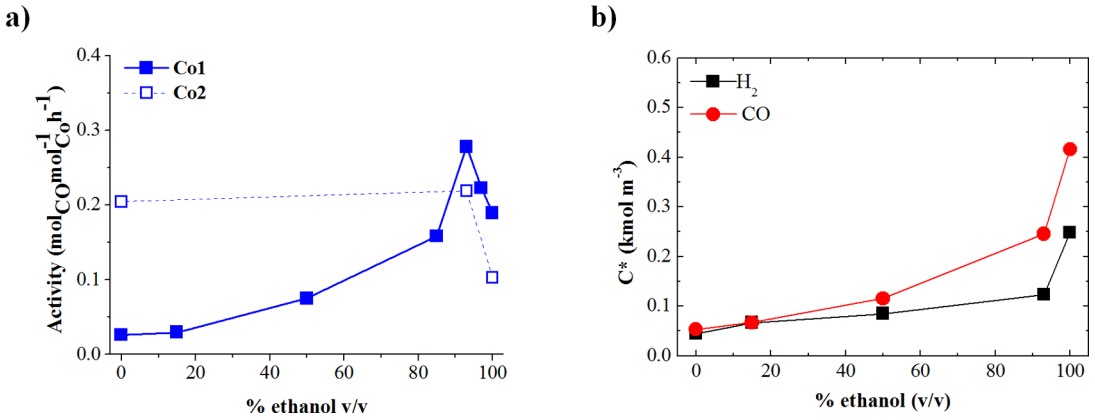

Figure 9. (a) Activity in $mol_{CO}\ mol_{Co}^{-1}\ h^{-1}$ of **Co1** and **Co2** NPs as a function of the percent ethanol. Conditions: 0.949 mmol Co, 30 bar $H_2/CO/Ar$ (2:1:0,15), 66 mL water, 1000 rpm, 180 °C, 12 h. (b) Solubility of H_2 and CO at 20 and 10 bar, respectively, and rt in heptane/water mixtures.

The detailed distributions of FT products formed during these catalytic experiments are described in Table 4.

Among the tested solvents, the highest activity was achieved in ethanol (up to 0.189 $mol_{CO}\ mol_{Co}^{-1}\ h^{-1}$), while for the other alcohols, FT activities between 0.027–0.053 $mol_{CO}mol_{Co}^{-1}\ h^{-1}$ were obtained. The results in longer alcohols could be explained by the competitive coordination of syngas and alcohols at the NPs surface, since high selectivity to acetals was observed in these solvents (Table 4).

The product selectivity was also affected by the chain length of the alcoholic solvents with high selectivity to C_{2+} when methanol, ethanol, and propanol were used with a maximum of 92% in ethanol. In contrast for longer chain alcohols, the selectivity decreased considerably (down to 56%) while the methane selectivity increased to ca. 30%. In all solvents, low CO_2 selectivity was observed, indicating low WGS activity under these conditions. Similarly, the hydrocarbon distribution showed high selectivity to C_{13+} in short chain alcohols, namely methanol and ethanol with a maximum of 67% in this latter solvent. For longer chain alcohols (Table 4, entry 3–5), this selectivity was lower (ca. 45%) with a shift to lighter products. These results can be correlated with the H_2:CO ratio measured in the gas phase at the end of the catalytic experiments, which increases with heavier alcohols due to acetal formation (Table 4). In light alcohols (entry 1 and 2), lower H_2:CO ratios were observed, resulting in low methane selectivity and high C_{13+} selectivity. In heavier alcohols, higher values were obtained, explaining the higher methane selectivity and the formation of short chain hydrocarbon products (Table 4, entry 4 and 5). In propanol, somewhat intermediate H_2:CO ratio and selectivity results were measured.

Interestingly, the catalysis in methanol exhibited a high olefin selectivity (65%) which decreased when the chain length of the alcohol increased, which was attributed to the lower H_2/CO ratio in the shorter alcohols that is in turn related to the lower amounts of acetals formed in these solvents.

As a conclusion, when alcohols are used as solvent for FTS, the formation of acetals catalyzed by CoNPs is observed together with hydrocarbon products. When the chain length of the alcoholic solvent increases, the formation of acetal progressively becomes the major process. In the case of short alcohols such as ethanol; however, high FT activity (up to 0.189 $mol_{CO}\ mol_{Co}^{-1}\ h^{-1}$) was observed with excellent product selectivity (80% hydrocarbons).

Optimization of the Composition of Ethanol/Water Mixtures. In view of the excellent results obtained using ethanol as the solvent, the influence of water was tested through a series of catalytic FT experiments in several water/ethanol mixtures using **Co1** and **Co2** as catalyst. The results in terms of activity are summarized in Figure 9a.

Comparing the activity obtained in pure water as the solvent, the increase in ethanol content from 0 to 93% resulted in a significant increase in the activity from 0.026 to 0.278 $mol_{CO}\ mol_{Co}^{-1}\ h^{-1}$. These results can be correlated to the increased solubility of syngas at higher ethanol content (Figure 9b).[31] At higher ethanol content, a decrease in the activity was observed to down to 0.189 $mol_{CO}\ mol_{Co}^{-1}\ h^{-1}$ due to the competitive formation of FT-acetals.

Importantly, in these experiments, acetal products (FT-acetals and Cn-acetals) were only detected when the content of water was ≤3%, which indicates that rapid hydrolysis of the acetals occurred at higher water content. To the best of our knowledge the activity observed for **Co1** when using 93% ethanol/water mixture (0.278 $mol_{CO}\ mol_{Co}^{-1}\ h^{-1}$) is the highest reported to date for an aqueous FT system using CoNPs synthesized by a colloidal method. This result

DOI: 10.1021/cs5020332
ACS Catal. 2015, 5, 4568–4578

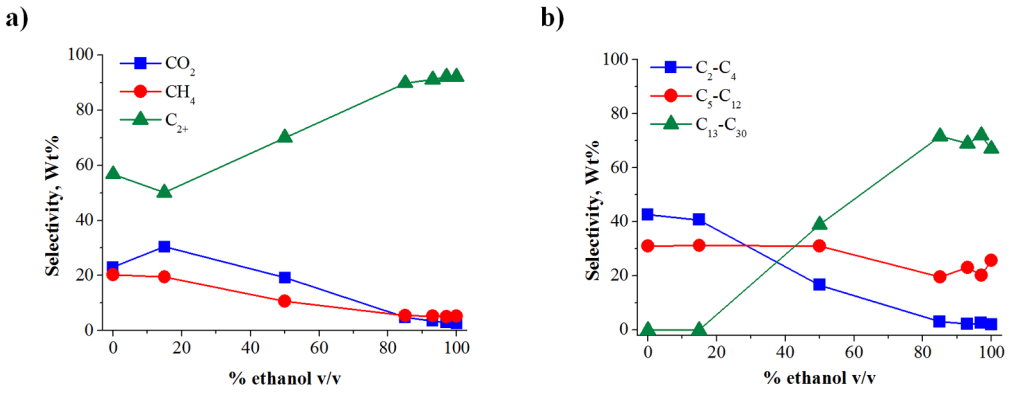

Figure 10. Selectivity (a) and hydrocarbon distribution (b) in wt % of FT experiments catalyzed by **Co1** NPs as a function of the % ethanol. Conditions: 0.949 mmol Co, 30 bar H_2/CO/Ar (2:1:0,15), 66 mL water, 1000 rpm, 180 °C, 12 h.

highlights the possibility to enhance the catalytic activity of a catalyst through the modification of their environment. XPS analysis of the used catalysts is displayed in the Supporting Information.

When **Co2** was used as the catalyst, similar activities were obtained in 93% ethanol/water mixture. As previously mentioned, the higher activities observed for **Co2** in water and hydrocarbon/water mixtures were attributed to its higher content in metallic cobalt when compared to **Co1**. In alcohols, however, similar activities were observed for both catalysts. As the reduction of cobalt salts was previously reported in alcohols at similar temperature,[32] it was concluded that the similar activities observed for both catalysts could be explained by the *in situ* reduction of **Co1** under these reaction conditions. In terms of selectivity (Figure 10a), the increase in ethanol content from 0 to ca. 90% led to a progressive increase in hydrocarbon selectivity from 57 to ca. 90% while the CO_2 and CH_4 selectivities decreased from 23 to 5% and from 20 to 5%, respectively. At higher ethanol content, these selectivities remained unchanged. It is noteworthy that in heptane/water mixtures, the increase in hydrocarbon selectivity was more accentuated than in ethanol/water mixtures, which can be explained by the rapid increase in syngas solubility when heptane is introduced compared to ethanol (Figure 7a vs Figure 9a).

The hydrocarbon products distribution (Figure 10b) was also clearly affected by the composition of the solvent. When the ethanol content was increased from 0 to 15%, no changes in selectivity were observed. However, at higher ethanol content, the product distribution was progressively shifted from short chain (C_{2-4}) to long chain hydrocarbons (C_{13-30}) with variation in selectivity from 40% to 0% and from 0% to 73%, respectively. Further increases in ethanol content did not affect these selectivities. Interestingly, while the solvent composition clearly affected the C_{2-4} and C_{13-30} selectivities, the relative amount of C_{5-12} hydrocarbon remained unchanged at ca. 25%. When **Co2** was used as the catalyst, the same selectivity trends were observed (Supporting Information).

These variations in product distribution, reflected in the variations in chain growth probability, can be rationalized by the changes in H_2:CO solubility ratio as a function of the ethanol content (Figure 11). Indeed, at ethanol contents up to 15%, an increase in H_2:CO solubility ratio was measured, resulting in the lowering of the α value and the formation of light products (C_{2-4} and C_{5-12}). At higher ethanol content, the H_2:CO solubility ratio decreased linearly, resulting in a

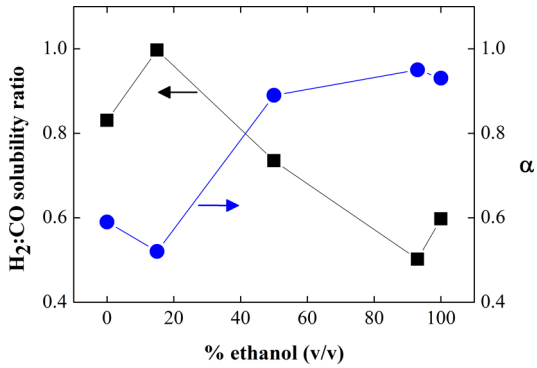

Figure 11. Measured H_2:CO solubility ratio and corresponding α values obtained for catalysis using different ethanol/water mixtures.

concomitant increase in the chain growth probability and thus, in a higher C_{13+} selectivity. These results again indicate that the main parameter governing the FT product distribution is the relative solubilities of H_2 and CO in these solvents.

Finally, from the comparison of **Co1** and **Co2** in the different solvent systems it is noteworthy that the presence of boron in **Co1** did not exhibit a clear effect in its catalytic performance.

CONCLUSIONS

The results described here show that the addition of cosolvents such as hydrocarbons and alcohols in AFTS strongly affects the selectivity and the FT product distribution. It was shown that the hydrocarbon distribution mainly depends on the solubility of syngas and on the H_2:CO ratio and can be tuned from light to heavy hydrocarbons with the selection of the appropriate aqueous solvent mixture.

In hydrocarbon/water mixtures, a compromise between the higher solubility of syngas in hydrocarbons and the better dispersion of the catalyst in water was revealed to be crucial to reach high activity and selectivity to C_{13+} hydrocarbons. No effect of the chain length (C_7–C_{16}) of the hydrocarbon cosolvents was observed on the selectivity of FTS while the activity was slightly affected. This also indicates that the presence of water and hydrocarbons at the surface of such Co nanocatalysts directly influences their selectivity in FTS by affecting their H_2/CO coverage. These results also suggest that the presence of water can significantly shorten the chain length of the hydrocarbons produced by FTS.

In alcohols, a significant effect was also observed; when the chain length of the alcoholic solvent increases, the formation of

DOI: 10.1021/cs5020332
ACS Catal. 2015, 5, 4568–4578

FT-acetal products progressively becomes the major process. In the case of short alcohols such as ethanol, however, high FT activity (up to 0.189 mol_{CO} mol_{Co}^{-1} h^{-1}) was observed with excellent product selectivity (90% hydrocarbons).

■ ASSOCIATED CONTENT

Supporting Information

The Supporting Information is available free of charge on the ACS Publications website at DOI: 10.1021/cs5020332.

Detailed experimental procedures, characterization data, and additional catalytic results. (PDF)

■ AUTHOR INFORMATION

Corresponding Authors

*E-mail cyril.godard@urv.cat. Fax: (+34) 977 559563 (C.G.).
*E-mail: carmen.claver@urv.cat (C.C.).

Notes

The authors declare no competing financial interest.

■ ACKNOWLEDGMENTS

The authors are grateful to Total S.A., the Spanish Ministerio de Economía y Competitividad (CTQ2013-43438-R and *Ramon y Cajal* fellowship to C.G.) and the Generalitat de Catalunya (2014SGR670) for financial support.

■ REFERENCES

(1) Calderone, V. R.; Shiju, N. R.; Curulla-Ferré, D.; Chambrey, S.; Khodakov, A.; Rose, A.; Thiessen, J.; Jess, A.; Rothenberg, G. *Angew. Chem., Int. Ed.* **2013**, *52*, 4397−4401.

(2) (a) Steynberg, A. In *Fischer−Tropsch Technology. Studies in Surface Science and Catalysis*; Steynberg, A., Dry, M., Eds.; Elsevier, Amsterdam, The Netherlands, 2006; Vol. *152*, p 1−3. (b) Dancuart, L. P.; Steynberg, A. In *Fischer−Tropsch synthesis, catalysts and catalysis*; Davis, B.H.; Occelli, M. L., Eds.; Elsevier: Eastbourne, UK, 2007; Vol. *163*, p 379−381. (c) Zhang, Q.; Kang, J.; Wang, Y. *ChemCatChem* **2010**, *2*, 1030−1058.

(3) Khodakov, A. Y. *Catal. Today* **2009**, *144*, 251−257.

(4) Gual, A.; Godard, C.; Castillón, S.; Curulla-Ferré, D.; Claver, C. *Catal. Today* **2012**, *183*, 154−171.

(5) Van Der Laan, G. P.; Beenackers, A. A. C. M. *Catal. Rev.: Sci. Eng.* **1999**, *41*, 255−318.

(6) (a) Hibbitts, D. D.; Loveless, B. T.; Neurock, M.; Iglesia, E. *Angew. Chem., Int. Ed.* **2013**, *52*, 12273−12278. (b) Claeys, M.; van Steen, E. *Catal. Today* **2002**, *71*, 419−427.

(7) Liu, X.; Linghu, W.; Li, X.; Asami, K.; Fujimoto, K. *Appl. Catal., A* **2006**, *303*, 251−257.

(8) Linghu, W.; Liu, X.; Li, X.; Fujimoto, K. *Catal. Lett.* **2006**, *108*, 11−13.

(9) Pendyala, V.; Jacobs, G.; Luo, M.; Davis, B. *Catal. Lett.* **2013**, *143*, 395−400.

(10) Xiao, C. X.; Cai, Z. P.; Wang, T.; Kou, Y.; Yan, N. *Angew. Chem., Int. Ed.* **2008**, *47*, 746−749.

(11) Wang, H.; Zhou, W.; Liu, J. X.; Si, R.; Sun, G.; Zhong, M. Q.; Su, H. Y.; Zhao, H. B.; Rodriguez, J. A.; Pennycook, S. J.; Idrobo, J. C.; Li, W. X.; Kou, Y.; Ma, D. *J. Am. Chem. Soc.* **2013**, *135*, 4149−4158.

(12) Wang, C.; Zhao, H.; Wang, H.; Liu, L.; Xiao, C.; Ma, D. *Catal. Today* **2012**, *183*, 143−153.

(13) Quek, X. Y.; Guan, Y.; van Santen, R. A.; Hensen, E. J. M. *ChemCatChem* **2011**, *3*, 1735−1738.

(14) Gual, A.; Delgado, J. A.; Godard, C.; Castillón, S.; Curulla-Ferré, D.; Claver, C. *Top. Catal.* **2013**, *56*, 1208−1219.

(15) Wang, H.; Kou, Y. *Chin. J. Catal.* **2013**, *34*, 1914−1925.

(16) Fan, X. B.; Tao, Z. Y.; Xiao, C. X.; Liu, F.; Kou, Y. *Green Chem.* **2010**, *12*, 795−797.

(17) (a) Scariot, M.; Silva, D. O.; Scholten, J. D.; Machado, G.; Teixeira, S. R.; Novak, M. A.; Ebeling, G.; Dupont, J. *Angew. Chem., Int. Ed.* **2008**, *47*, 9075−9078. (b) Silva, D. O.; Scholten, J. D.; Gelesky, M. A.; Teixeira, S. R.; Dos Santos, A. C. B.; Souza-Aguiar, E. F.; Dupont, J. *ChemSusChem* **2008**, *1*, 291−294.

(18) Yan, N.; Zhang, J. G.; Tong, Y.; Yao, S.; Xiao, C.; Li, Z.; Kou, Y. *Chem. Commun.* **2009**, 4423−4425.

(19) Silva, D. O.; Luza, L.; Gual, A.; Baptista, D. L.; Bernardi, F.; Zapata, M. J. M.; Morais, J.; Dupont, J. *Nanoscale* **2014**, *6*, 9085−9092.

(20) (a) Bligaard, T.; Nørskov, J. K.; Dahl, S.; Matthiesen, J.; Christensen, C. H.; Sehested, J. *J. Catal.* **2004**, *224*, 206−217. (b) Khodakov, A. Y.; Chu, W.; Fongarland, P. *Chem. Rev.* **2007**, *107*, 1692−1744. (c) Schulz, H. *Appl. Catal., A* **1999**, *186*, 3−12.

(21) (a) Wu, Chuan; Pang, Chun Hui; Wu, Feng; Bai, Ying; Chen, Chi; Zhong, Y. *Adv. Mater. Res.* **2011**, *391−392*, 1085. (b) Mitov, M.; Popov, A.; Dragieva, I. *J. Appl. Electrochem.* **1999**, *29*, 59−63. (c) Petit, C.; Wang, Z. L.; Pileni, M. P. *J. Phys. Chem. B* **2005**, *109*, 15309−15316.

(22) Dry, M. E. *J. Mol. Catal.* **1982**, *17*, 133.

(23) Pray, H. A.; Schweickert, C. E.; Minnich, B. H. *Ind. Eng. Chem.* **1952**, *44*, 1146−1151.

(24) Matsumoto, D. K.; Satterfield, C. N. *Ind. Eng. Chem. Process Des. Dev.* **1985**, *24*, 1297−1300.

(25) Florusse, L. J.; Peters, C. J.; Pàmies, J. C.; Vega, L. F.; Meijer, H. *AIChE J.* **2003**, *49*, 3260−3269.

(26) Deimling, A.; Karandikar, B. M.; Shah, Y. T.; Carr, N. L. *Chem. Eng. J.* **1984**, *29*, 127−140.

(27) Fan, X. B.; Yan, N.; Tao, Z. Y.; Evans, D.; Xiao, C. X.; Kou, Y. *ChemSusChem* **2009**, *2*, 941−943.

(28) Carey, F. A.; Sundberg, R. J. *Organic chemistry*, 4th ed.; McGraw-Hill: New York, 2000; pp 449−452.

(29) Gunanathan, C.; Shimon, L. J. W.; Milstein, D. *J. Am. Chem. Soc.* **2009**, *131*, 3146−3147.

(30) *CRC Handbook of Chemistry and Physics*, Internet Version, 86th ed.; CRC: Boca Raton, FL, 2006; http://www.hbcpnetbase.com.

(31) Purwanto; Deshpande, R. M.; Chaudhari, R. V.; Delmas, H. *J. Chem. Eng. Data* **1996**, *41*, 1414−1417.

(32) (a) Fiévet, F.; Brayner, R. In *Nanomaterials: A Danger or a Promise?*; Brayner, R., Fiévet, F., Coradin, T., Eds.; Springer: London, 2013; p 1−25. (b) Montiel, M. G.; Santiago-Jacinto, P. P.; Góngora, J. A. I. D.; Reguera, E.; Gattorno, G. R. *Nano-Micro Lett.* **2011**, *3*, 12−19.

DOI: 10.1021/cs5020332
ACS Catal. 2015, 5, 4568−4578